A heat pretreatment method to improve the RT-qPCR detectability of plasmid-borne antibiotic resistance genes in environmental samples

Fan, L.; Zhang, T.; Zhou, T.; Yang, H.; Cheng, F.; Qu, J.; ... ; Peijnenburg, W.J.G.M.

ACS ES&T Water

pubs.acs.org/estwater

Article

A Heat Pretreatment Method to Improve the RT-qPCR Detectability of Plasmid-Borne Antibiotic Resistance Genes in Environmental Samples

Linyi Fan, Tingting Zhang, Tong Zhou, Hao Yang, Fangyuan Cheng, Jiao Qu, Ya-nan Zhang,* and Willie Peijnenburg

Cite This: *ACS EST Water* 2025, 5, 4025−4034

Read Online

ACCESS | Metrics & More | Article Recommendations | Supporting Information

ABSTRACT: The dissemination of antibiotic resistance genes (ARGs) has garnered significant attention. Our study revealed that nearly 90% of the supercoiled form plasmids in laboratory standard ARGs vector plasmids were undetectable by direct detection using Quantitative Real-time polymerase chain reaction (qPCR). We propose a pretreatment heating at 75 °C for 10 min to enhance the efficiency of qPCR detection for plasmid borne ARGs. Treatment of the pBR322 plasmid using this method enhanced the qPCR detectability of *tet*A (carried by pBR322 plasmid) from 14.1% to 69.1%. Subsequently, we extracted DNA from water samples collected from the Songhua River and compared the relative abundance of ARGs in the samples before and after the heat pretreatment. The results revealed that the relative abundance of approximately 56% of the ARGs increased, the majority of which are located on plasmids. This finding indicates that direct detection using qPCR could lead to an underestimation of the levels of contamination associated with plasmid-borne ARGs. In addition, we investigated that the change of vector plasmid structure in the ARGs degradation experiment can seriously interfere with the qPCR quantification of ARGs, thereby presenting a challenge to accurately assessing the degradation rate of ARGs.

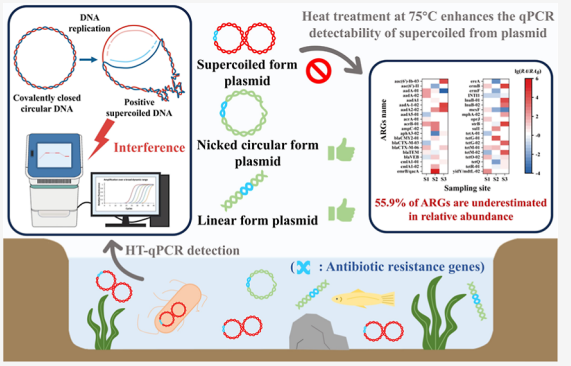

KEYWORDS: *antibiotic resistance gene, supercoiled form plasmid, qPCR, heat treatment*

INTRODUCTION

The issue of antimicrobial resistance arising from antibiotic misuse has garnered extensive global attention.[1] Although the emergence of antimicrobial resistance is a natural process, it has been significantly accelerated by the extensive use of antibiotics in healthcare and aquaculture, leading to the proliferation of antibiotic-resistant bacteria (ARB).[2,3] From 2000 to 2015, global antibiotic use increased by 65% and is projected to reach 128 billion defined daily doses (DDDs) by 2030.[4] There is a significant correlation between the emergence of antibiotic resistance genes (ARGs) and antibiotic concentrations. For instance, the relative abundance of *sul1* and *sul2* in river sediments is positively correlated with sulfonamide concentrations in river water.[5] Thus, the misuse of antibiotics exacerbates the contamination level of ARGs in the environment. An analysis utilizing Natural Language Processing (NLP) identified 9374 studies reporting ARG contamination across various regions.[6] Among these, multidrug resistance was the most frequently documented, followed by β-lactams, glycopeptides, sulfonamides, and tetracyclines. Survey statistics indicate that the relative abundance of ARGs in the environment was 10^{-2}−10^{-7} copies/16S rRNA, and the relative abundance of *tet*D in the Altamaha River estuary is even as high as 1.48×10^{-1} copies/16S rRNA.[7]

Horizontal gene transfer (HGT) is a key factor contributing to the rising levels of ARG contamination, encompassing four modes: conjugation transfer, transformation, transduction, and vesicular transport.[8,9] Mobile genetic elements (MGEs) serve as vectors of ARGs and play crucial roles in HGT.[10] For instance, integron can capture and integrate exogenous genes, converting them into functional gene expression units which facilitate the transfer of multidrug-resistant genes in bacteria via transposons or plasmids.[11] The ARGs in the latest PLSDB database were quantified using AMRFinderPlus, identifying a total of 96,072 ARGs across 59,895 complete plasmid sequences. This implies that each plasmid contains approximately 1.6 ARGs on average.[12] Moreover, research in the

Received: March 9, 2025
Revised: June 24, 2025
Accepted: June 26, 2025
Published: June 29, 2025

https://doi.org/10.1021/acsestwater.5c00272
ACS EST Water 2025, 5, 4025−4034

medical field has shown that the most clinically significant ARGs are often located on various MGEs and can be transmitted between both pathogenic and nonpathogenic organisms.[13] Therefore, accurately identifying and quantifying plasmid-borne ARGs is essential.

However, as one of the primary tools for ARGs detection, qPCR may not be capable of directly detecting plasmid-borne ARGs. As early as 1992, Garner and Chrambac discovered three forms of the pBR322 plasmid:a negative supercoiled form (hereafter referred to as supercoiled form), a nicked circular form, and a linear form, while it was also detected that the migration distances of the pBR322 plasmid in these different conformations vary during electrophoresis.[14,15] Subsequently, other scholars identified the fourth structure of pBR322, known as the relaxed circular form. Researchers have determined that supercoiled form plasmids are poor substrates for qPCR.[16] This is because covalently closed circular DNA generates a positive supercoiled form when analyzed by qPCR, which inhibits the breaking of DNA double strands and prevents DNA replication.[17] In contrast, nicked circular and linear form plasmids are suitable substrates for qPCR because they lack a complete loop structure and cannot form a positive supercoil. This observation has also been noted in the literature concerning ARGs degradation, as most ARGs studied in the laboratory are carried by plasmids.[18,19]

High-Throughput qPCR (HT-qPCR) is an advanced technology in real-time quantitative polymerase chain reaction that integrates automated equipment, microfluidic chips, or multiwell plate technology. This integration facilitates rapid and precise large-scale quantitative analysis of samples or target genes. Owing to its advantages of low cost, high sensitivity, high specificity, and high throughput, this technique is widely employed for detecting ARGs in environmental samples.[20−22] Zhuang et al. conducted a Natural Language Processing (NLP) analysis of papers related to ARG contamination detection and provided a detailed list of 40 papers, 29 of which employed qPCR/PCR methods.[6] Currently, the accuracy of qPCR in detecting plasmid DNA remains uncertain. Given that a substantial number of ARGs in the environment are found on plasmids, which exhibit higher transmissibility,[23] accurate quantification of plasmid-borne ARGs is essential for assessing both their ecological impact and potential human health risks.

This study assessed the detectability of laboratory standard ARG vector plasmids using qPCR. Simultaneously, we proposed a sample pretreatment method designed to nonspecifically enhance the detection efficiency of qPCR for plasmid-borne ARGs. This method was employed to detect and analyze ARGs in river water samples from the Songhua River located in northeast China, revealing significant changes in ARGs abundance before and after treatment. Our findings demonstrate that direct detection of ARGs using qPCR in the environment substantially underestimates contamination levels of plasmid-borne ARGs.

We finally discuss that when plasmid-borne ARGs are utilized in photodegradation experiments, the experimental samples could not be accurately quantified by qPCR. This leads to a paradoxical trend of increasing ARGs concentrations in the early stages of degradation, complicating the accurate analysis of the degradation rate of ARGs. Consequently, we propose utilizing nucleic acid endonuclease to construct linear form ARGs vector plasmids for degradation experiments to ensure data accuracy.

METHODS AND MATERIALS

Plasmids and Nucleic Acid Endonucleases. The pBR322 plasmid (0.5 g/L) containing the tetracycline resistance gene *tet*A and the pUC57 plasmid (0.5 g/L) containing the ampicillin resistance gene *Amp*R, were purchased from Thermo Fisher Scientific and Sangon Biotech Co., Ltd. (Shanghai, China), respectively. The nucleases ApaL I and *Sma*I, used for the construction of linear form plasmids, were purchased from BBI Life Sciences Corporation. The nuclease Nt.BstNBI used to construct the nicked circular form plasmid was purchased from Beyotime Biotechnology. Additional chemicals, reagents, materials, and their corresponding commercial suppliers are listed in Text S1 of the Supporting Information.

Construction of Linear, Relaxed Circular and Nicked Circular Form Plasmids. Linear form pBR322 was constructed using ApaL I nuclease, which has a single cleavage site (5′-G↓TGCAC-3′, 3′-CACGT↑G-5′). The digestion system comprised 16 μL of nuclease-free water, 2 μL of 10× Buffer Y, 1 μL of DNA (0.1 μg/μL) and 0.5 of μL ApaL I (10 U/μL). After gentle mixing and brief shaking, the mixture was incubated at 37 °C for 2 h. Similarly, linear pUC57 was constructed using *Sma*I endonuclease, which has a single cleavage site (5′-CCC↑GGG-3′, 3′-GGG↓CCC-5′). The enzymatic procedure for *Sma*I was identical to that employed for ApaL I.

Relaxed circular form of pBR322 and pUC57 were constructed using cowpox DNA topoisomerase I. This enzyme catalyzes the breaking and rejoining of phosphodiester bonds at specific sequences in single-stranded regions within double-stranded DNA, leading to the relaxation of both positive and negative supercoiled forms of covalently closed circular DNA.[24,25] The reaction mixture consisted of 15 μL nuclease-free water, 2 μL 10× reaction buffer, 2 μL DNA (50 ng/μL), and 1 μL cowpox DNA topoisomerase I (1 U/μL). After gentle mixing and brief shaking, the mixture was incubated at 37 °C for 2 h.

Nicked circular form plasmid was constructed using the Nt.BstNBI enzyme. The digestion system comprised 16 μL of nuclease-free water, 2 μL of 10× Buffer O, 1 μL of DNA (0.1 μg/μL) and 0.5 of μL ApaL I (10 U/μL). After gentle mixing and brief shaking, the mixture was incubated at 55 °C for 1 h. It is worth noting that relaxed circular and nicked circular form plasmids represent distinct topological forms. The fundamental structural difference involves strand continuity: relaxed circular plasmids preserve complete double-stranded integrity, while nicked circular form plasmids contain a single-strand nick, resulting in an interrupted phosphodiester backbone in one DNA strand.

qPCR Standard Curve for ARGs. The ARGs solution was serially diluted to prepare concentrations of 10 mg/L, 1 mg/L, 0.1 mg/L, 10 μg/L, and 1 μg/L. The prepared solutions were analyzed using qPCR to obtain the corresponding Ct values, with three parallel assays conducted for each sample group. Standard curve equations were constructed for ARG concentration against Ct values, yielding an R^2 value of 0.999.

DNA Electrophoresis and Fluorescence Signal Analysis. DNA electrophoresis is a valuable technique for plasmid structure analysis. For example, electrophoresis can be used to analyze the pBR322 plasmid through electrophoretic bands, identifying structures such as supercoiled form (4500 bp), nicked circular form (>5000 bp), linear form (between

https://doi.org/10.1021/acsestwater.5c00272
ACS EST Water 2025, 5, 4025−4034

supercoiled and nicked circular form), and single-linear form (2000 bp).[15]

Half a gram of 1% agarose was dissolved in 50 mL of TAE buffer solution and microwaved until completely dissolved. An amount of 2.5 μL of 4S Green Plus nontoxic nucleic acid dye was added to the solution, and allowed to cool to form an electrophoresis gel. In each sample well, 1 μL of 6× Glycerol Gel Sampling Buffer VII mixed with 5 μL of ARGs sample was added. Electrophoresis was conducted at 120 V for 20 min using DNA Marker S (100−5000 bp) as a molecular weight standard. Electropherograms were captured using an electrophoresis gel imaging system.

ImageJ software facilitates precise quantification of fluorescence signals specifically emanating from targeted areas in electropherogram analyses.[26] The area and average fluorescence intensity of the bright regions were identified and measured. The total fluorescence was calculated as the product of the area and the average fluorescence intensity, representing the number of DNA molecules in the region.

Heat Pretreatment of Plasmid Samples. First, added 90 μL of plasmid DNA sample to a 200 μL PCR tube and heated at 75 °C for 10 min in a thermostatic metal bath. Immediately cooled the tubes in an ice bath. Subsequently, added 5 μL of 200 mM Tris−HCl solution and 5 μL of 20 mM EDTA solution to achieved final concentrations of 10 mM Tris−HCl and 1 mM EDTA, respectively, to prevent DNA degradation during storage. Stored the treated samples at −20 °C.

DNA AFM Image. The damage to DNA after exposure to light was observed using atomic force microscopy (AFM).[27,28] Applied 1 mL of a 10 ng/μL DNA sample onto a mica sheet. Allowed the droplet to dry nearly completely, then blotted away the excess liquid with filter paper. Once the sample was completely dry, proceeded with testing on the machine. Imaging was performed using a Dimension ICON instrument, scanned with an Otespa-r3 probe in contact mode at a scanning speed of 1 Hz. AFM images were analyzed using Nano Scope Analysis 1.8 software to measure DNA length.

Extraction and Analysis of ARGs in Songhua River Water Samples. We collected water samples from the Songhua River located in northeast China in August. The sampling sites are illustrated in Figure S1, and their coordinates are listed in Table S3. Water samples were collected at a depth of 0.5 m using a water sampling bucket, transferred into sterile bio sampling bags, and then transported to the laboratory for storage at 4 °C. Sample DNA was extracted, and high-throughput detection of target ARGs was conducted using the QuantStudio 12 K Flex (Applied Biosystems). Relative abundance (RA) was calculated using the equation $2^{-\Delta Ct}$, where $\Delta Ct = Ct$ (target gene) − Ct (internal reference gene).

RESULTS AND DISCUSSION

Plasmid-Borne ARGs Cannot be Fully Detected by qPCR. The structure of the ARGs vector plasmid may interfere with ARG detection by qPCR. We utilized the ApaL I endonuclease to create the linear form pBR322 plasmid (*tet*A vector plasmid), which linearized the plasmid without impacting the ARGs. The *tet*A standard curves were generated using the *tet*A vector plasmid both before and after linearization as the qPCR reaction substrate: the qPCR methods and primers are detailed in Text S2 and Table S1. The results indicated that ARGs utilizing the linearized pBR322 plasmid as a vector exhibited lower Ct values (Figure 1a). The analysis of the two standard curves presented in

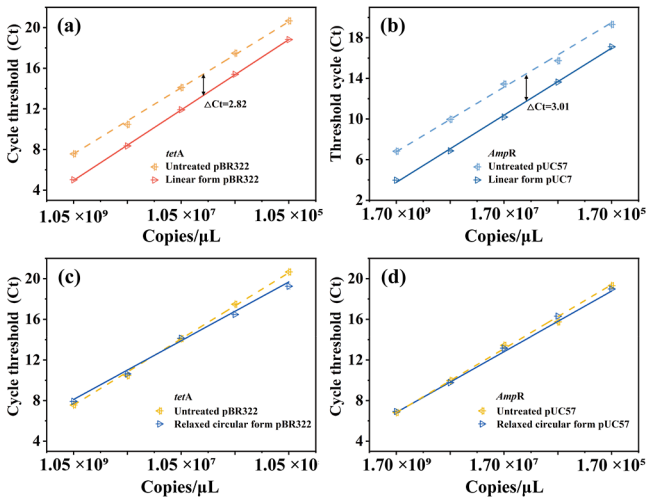

Figure 1. Variations in ARGs qPCR standard curves observed before and after the digestion of pBR322 (a) and pUC57 (b) plasmids. Variations in ARGs qPCR standard curves observed before and after the despiralization of pBR322 (c) and pUC57 (d) plasmids. The standard curve equations are listed in Table S2.

Figure 1a revealed that the difference in intercept between the two sets of equations (ΔCt[29]) was 2.82. This suggests that the concentration of *tet*A detected following the linearization of the pBR322 plasmid was 7.06-fold higher compared to that of the untreated plasmid, if quantified using a standard curve generated using linear form plasmids. Since linear form plasmids serve as excellent templates for qPCR, the standard curve generated using linear form plasmids as vectors can accurately determine the actual concentration of tetA genes.[16] This indicated that only 14.1% of the untreated pBR322 plasmid can be directly detected by qPCR (The calculations are detailed in Text S5). The experiments were repeated using *Sma*I endonuclease to construct a linear pUC57 plasmid (*Amp*R vector plasmid). It was found that only 12.4% of the untreated pUC57 plasmid could be directly detected by qPCR (Figure 1b).

ARGs Carried by Supercoiled Form Plasmids are Poor Substrates for qPCR. To identify which plasmids in the standard plasmid samples could not be directly detected by qPCR, we employed electrophoresis to analyze the standard pBR322 and pUC57 plasmid samples, which revealed a high prevalence of the supercoiled form and a small fraction of the nicked circular form. After treatment with nucleic acid endonuclease, all plasmids converted to the linear form (Figure 2a,b). To analyze the proportion of plasmids with supercoiled and nicked circular form in the samples, we quantified the fluorescence signals of the plasmid bands in the electropherograms using ImageJ software. The results indicated that the nicked circular form in the standard pBR322 and pUC57 plasmids accounted for only 12.6 and 10.9% of the total plasmids. This proportion closely resembles the 9% finding by Shin and Lee, underscoring the widespread presence of plasmids exhibiting nicked circular form.[26] These percentages closely align with the quantifiable proportion in the standard plasmids, which are 14.1 and 12.4% for pBR322 and pUC57, respectively. Subsequently, we simulated the qPCR predenaturation process for the pBR322 plasmid. Heating at 95 °C for 1 min left the supercoiled form largely unchanged, while the original nicked circular form was converted into single-stranded DNA (Figure 2c), enabling it

https://doi.org/10.1021/acsestwater.5c00272
ACS EST Water 2025, 5, 4025−4034

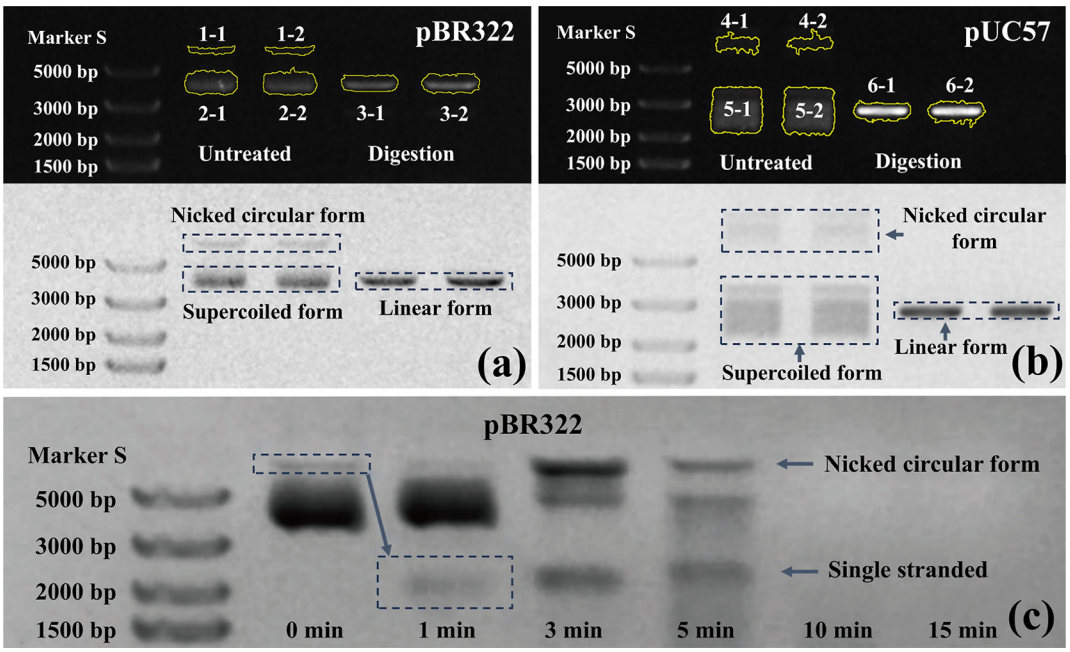

Figure 2. Electropherograms of pBR322 (a) and pUC57 (b) plasmid before and after enzymatic treatment (The numbering of fluorescence regions corresponds to the fluorescence intensity data in Table S4. For instance, Region 1 is indicative of the pBR322 plasmid in its Nicked circular form, where subregions 1−1 and 1−2 are configured to be parallel to one another. This pattern of arrangement applies to the remaining regions as well). Structure change of pBR322 plasmid after heating treatment at 95 °C (c).

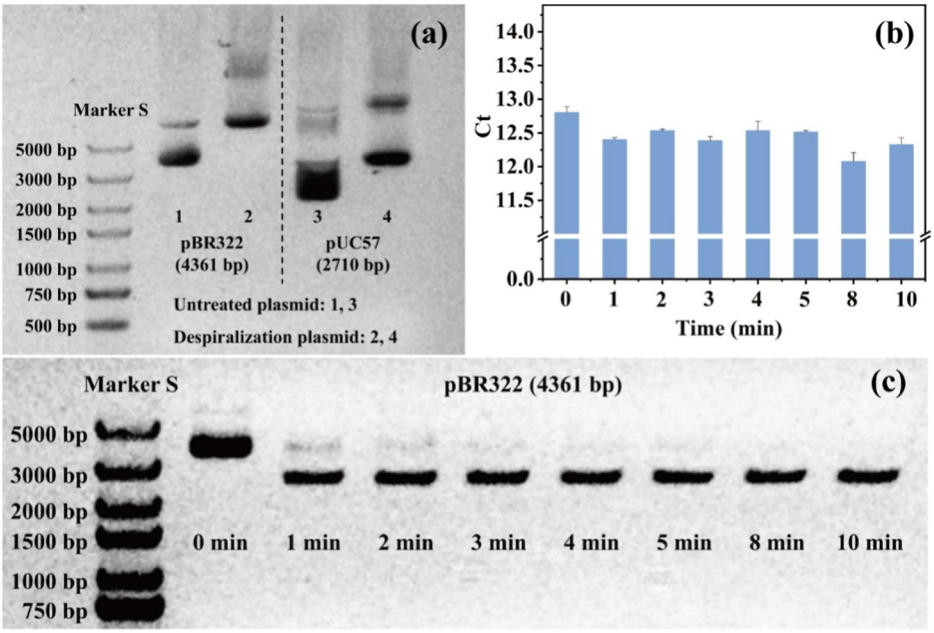

Figure 3. Electrophoretic strips of plasmid DNA after deconvolution by topoisomerases (a). Effect of treatment of pBR322 plasmid with 0.2 M NaOH on *tet*A qPCR *Ct* value (b). Electrophoretic bands of pBR322 plasmid after different times of treatment with 0.2 M NaOH (c).

to bind to the primer and facilitate subsequent DNA replication. However, the supercoiled form of the plasmid was not effectively deconvoluted, which impeded the DNA replication process and ultimately reduced the qPCR detection efficacy of the plasmid.[30,31] We constructed the nicked circular form plasmid using the nicking enzyme Nt.BstNBI. It was observed that at identical concentrations, the Cq value of the nicked circular pBR322 was significantly lower than that of the untreated pBR322. This behavior was similar to that of the linearized plasmid, demonstrating that the nicked circular form plasmid is an effective substrate for qPCR (Figures S6 and S7).

This finding suggests that the structure of ARGs vector plasmids has a non-negligible influence in qPCR. ARGs vector plasmids found in the environment are typically present in their supercoiled form.[32] Given the widespread use of HT-qPCR for detecting environmental ARGs, it is essential to assess whether employing HT-qPCR for the direct detection of environmental samples results in an underestimation of plasmid-borne ARGs contamination levels. This work was

https://doi.org/10.1021/acsestwater.5c00272
ACS EST Water 2025, 5, 4025−4034

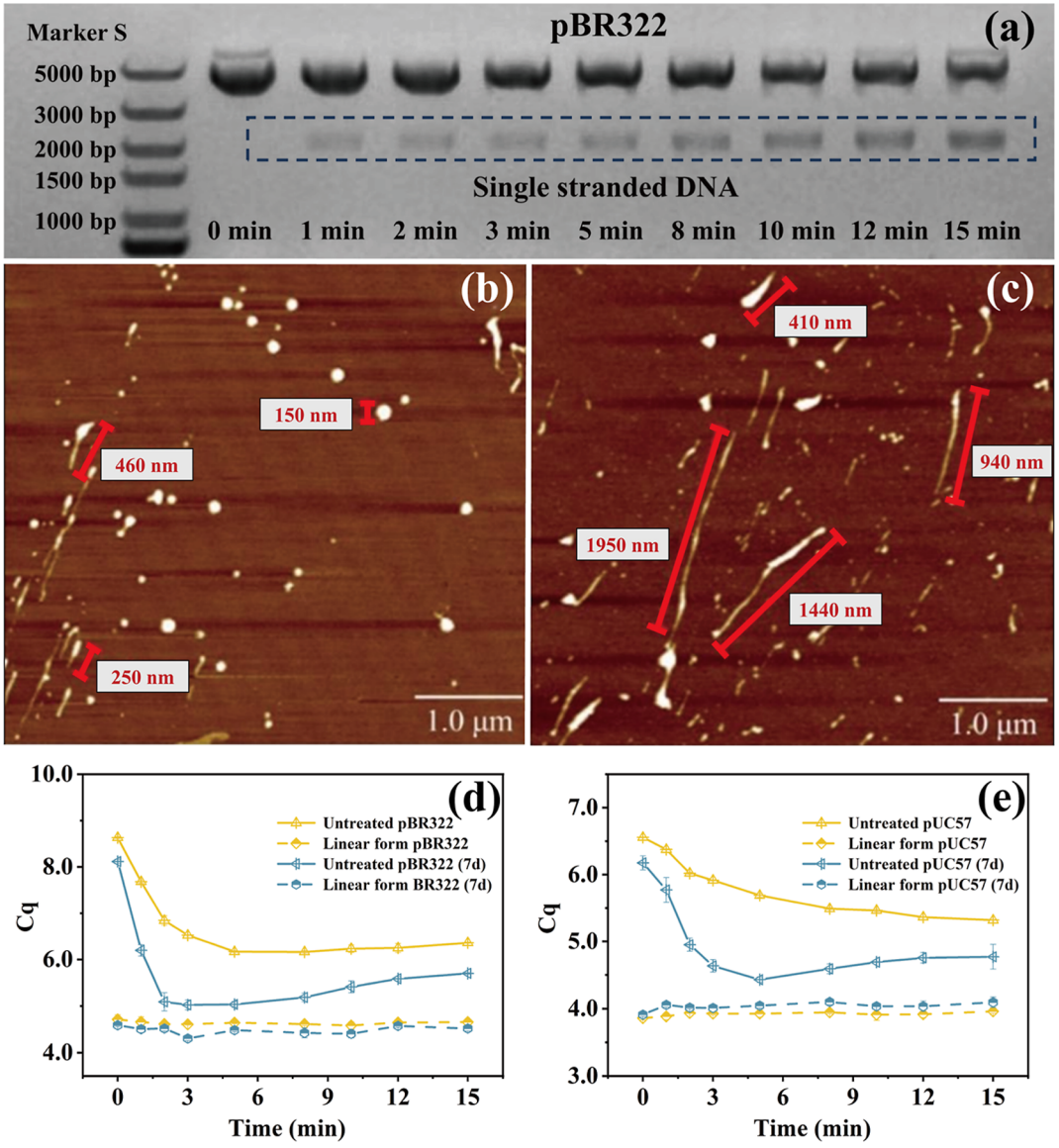

Figure 4. Structure change of pBR322 plasmid under heating at 75 °C (a). AFM images of pBR322 plasmid before (b) and after (c) treatment at 75 °C for 10 min. Effect of different 75 °C heating treatment times on pBR322 (d) and pUC57 (e) plasmid qPCR detection (Untreated plasmid: commercial plasmid not subjected to enzyme treatment; Linear form plasmid: commercial plasmid that has undergone enzyme treatment). The stability of the heat pretreatment samples was assessed after storage at −20 °C for 7 days (indicated by the blue line in the figure).

very challenging due to our inability to utilize enzymatic processing on plasmids of unknown sequences found in the environment. Therefore, it is essential to develop a nonspecific enhancement for the processing of supercoiled form plasmids to enhance their detectability by qPCR.

Disruption of the Covalently Closed Loop Structure of Vector Plasmids is Crucial for Enhancing the qPCR Quantifiability of ARGs. To develop a method for nonspecifically enhancing the qPCR quantifiability of plasmid-borne ARGs, we explored the use of topoisomerases and NaOH base denaturation. These methods are designed to disrupt the supercoiled form of plasmids. In bacteria, type I and type II topoisomerases are capable of relaxing negative as well as positive supercoiled form of plasmids by cleaving and rejoining the DNA double strands.[33,34] This facilitates the unspooling and successful replication of plasmid DNA.[35] We attempted to utilize cowpox topoisomerase I to relax the supercoiled form of the pBR322 and pUC57 plasmids. Electrophoretic analysis of the treated samples demonstrated significant upward shifts in the electrophoretic bands of the plasmids, indicating that the plasmid structures had relaxed, thereby confirming the successful construction of plasmids in a relaxed circular form (Figure 3a). The standard curve for qPCR was established using the ARGs carried by the relaxed circular form plasmid as the substrate, and it was found that there was no significant difference when compared to the untreated plasmid (Figure 1c,d), confirming that the relaxed circular form plasmid was also a poor substrate for qPCR.

Given that certain chemicals can denature DNA, we attempted to generate single-stranded DNA by breaking the hydrogen bonds of plasmid DNA using NaOH (Text S6).[36−38] When treating pBR322 with varying NaOH concentrations, we observed denaturation beginning at 0.2 M NaOH (Figure S2). The denatured plasmid band appeared between the supercoiled form plasmid and the single-stranded DNA bands, forming a new band. Studies by some scholars indicate that

https://doi.org/10.1021/acsestwater.5c00272
ACS EST Water 2025, 5, 4025−4034

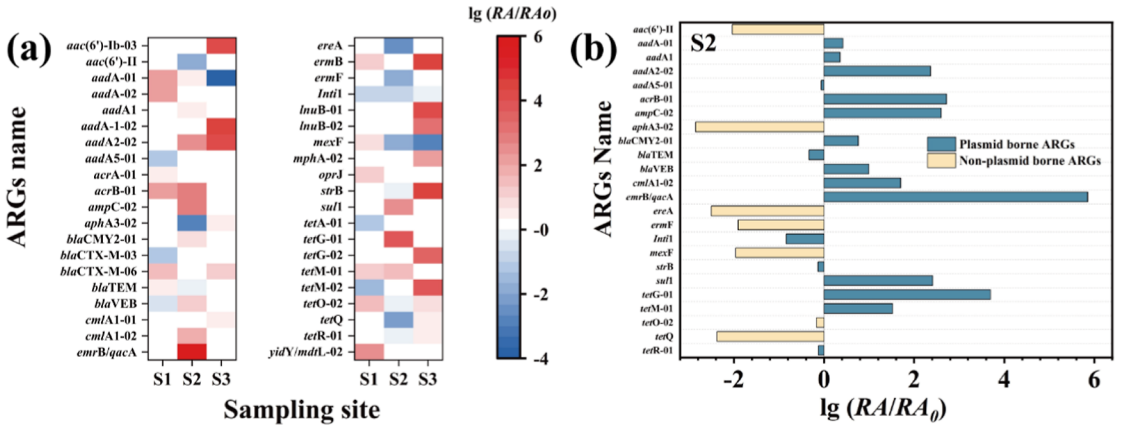

Figure 5. Changes in the relative abundance of ARGs before and after heat pretreatment of DNA samples from the Songhua River (a). Validation of the location of ARGs in S2 samples (b). (RA_0: relative abundance of untreated samples; *RA*: relative abundance of treated samples; Variations in Relative Abundance before and after treatment, represented by lg (RA/RA_0)).

while NaOH effectively cleaves hydrogen bonds within DNA, enabling the transition to single-stranded DNA, its efficacy is primarily observed in linear DNA. Plasmid DNA presents a distinct scenario as its structural extremities, the 3′ and 5′ ends, are fortifyingly connected through covalent bonds, impervious to NaOH-induced cleavage. Thus, plasmid DNA, when exposed to NaOH, indeed transitions to a single-stranded state; however, the single strands remain joined due to these robust covalent bonds. Upon re-exposure to neutral pH, complementary base pairing facilitates the reformation of the double-stranded DNA, engendering a new topological form of the plasmid. This transition manifests prominently as a pronounced downward shift in the electrophoretic band patterns.[39] To evaluate whether this new structure facilitates plasmid DNA deconvolution, we treated pBR322 with 0.2 M NaOH and observed that the structure remained stable with extended treatment durations (Figure 3c). Subsequent qPCR assays indicated that this new structure did not enhance the efficiency of qPCR detection of *tet*A carried by the pBR322 plasmid (Figure 3b). Therefore, the interference of the plasmid structure with qPCR may only be resolved by disrupting the intact circular structure of the plasmid and mitigating the generation of twisting stresses.

Heat Treatment at 75 °C Nonspecifically Enhances the qPCR Detectability of Plasmid-Borne ARGs. Literature states that DNA can be partially denatured at temperatures above 50 °C, resulting in disruption of hydrogen bonding.[40] In our experiments, we observed that heat treatment at 75 °C effectively eliminated the supercoiled form of the pBR322 plasmid, whereas prolonged heating (more than 3 min) at 95 °C resulted in significant damage to the plasmid (Figure S3). Electrophoretic analysis of pBR322 plasmid samples after heat treatment at 75 °C indicated that the quantity of single-stranded DNA increased significantly with prolonged treatment time. Concurrently, the bands corresponding to the supercoiled form shifted slightly upward, indicating that some plasmids had converted into their linear form (Figure 4a). To visualize the structure change of the pBR322 plasmid more intuitively, we examined the morphology of the plasmid in the samples using atomic force microscope (AFM). The results revealed that most of the plasmid in the untreated samples appeared as compact globules. These globules had diameters of approximately 150 nm (Figure 4b), indicating that the DNA existed in a supercoiled form.[41] In contrast, the samples subjected to heat treatment at 75 °C for 10 min exhibited numerous linear form plasmids with lengths exceeding 1000 nm (Figure 4c), demonstrating that the heat treatment caused plasmid breakage and the formation of linear form and single-stranded plasmids. Heat treatment serves a dual function in plasmid DNA alteration: first, it induces substantial denaturation of plasmid DNA, resulting in the collapse of single-stranded regions;[40] second, it disrupts hydrogen bonds within the DNA double helix, thereby compromising its structural integrity and rendering the DNA more vulnerable to hydrolytic and oxidative damage. Consequently, these effects facilitate the transition of plasmid DNA to its linear form and contribute to the production of substantial quantities of linear and single-stranded DNA. This subset of linear form plasmids and the single-stranded DNA were suitable substrates for qPCR amplification. Although this method does not completely eliminate the supercoiled form of the plasmid, the ratio of such structures is significantly reduced.

The results of the qPCR detection indicated that the concentration of *tet*A detected in the samples increased gradually with the duration of heat treatment at 75 °C. However, the increase in the quantifiable rate of plasmid-borne ARGs during heat treatment reaches a plateau period. Specifically, pBR322 enters the plateau period at 6 min, while the pUC57 plasmid does so after 10 min. Based on these observations, we selected 10 min as the optimal duration for heat treatment. After 10 min of treatment, the detected concentration of *tet*A rose 4.90-fold (Figure 4d), indicating that this method enhanced the proportion of the detectable fraction of the pBR322 plasmid from 14.1 to 69.1%. Similarly, treatment of the pUC57 plasmid using this method increased the detected concentration of *Amp*R by 2.16-fold (Figure 4e), suggesting that the method has a certain degree of general applicability.

To verify the stability of the heat-treated samples, we stored them at −20 °C for 7 days. Following storage, we conducted qPCR again and observed that the detected concentrations of both *tet*A and *Amp*R increased during exposure from 0 to 10 min (Figure 4d,e). This increase may be attributed to damage of the supercoiled form plasmid caused by freezing and thawing, which likely resulted in the formation of some nicked circular and linear form plasmids.[42,43] In conclusion, this method nonspecifically enhanced the qPCR detectability of

https://doi.org/10.1021/acsestwater.5c00272
ACS EST Water 2025, 5, 4025−4034

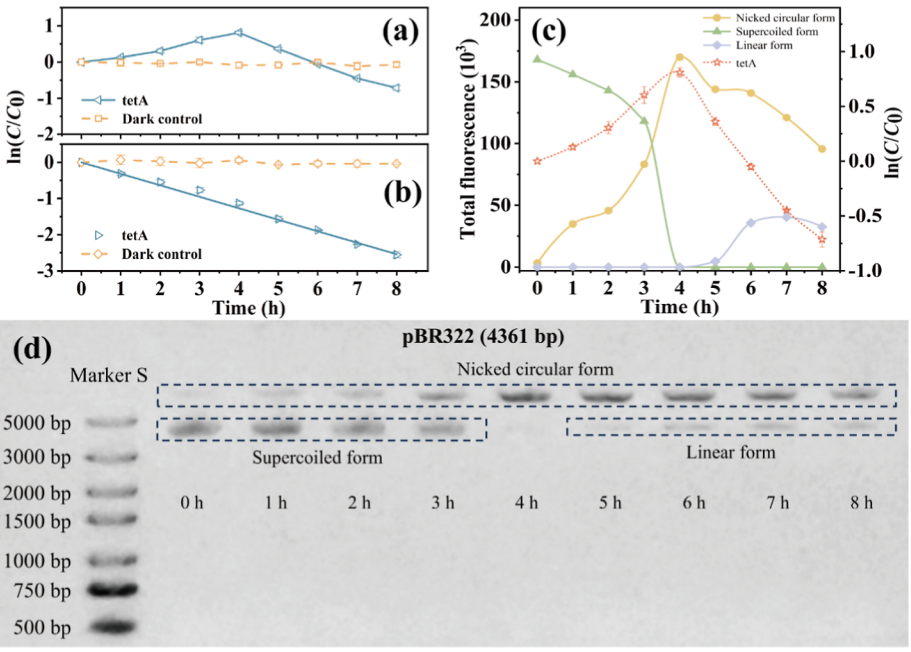

Figure 6. Kinetics of *tet*A photodegradation carried by pBR322 plasmid before (A) and after (B) digestion (C is the concentration of *tet*A at the given time point, C_0 is the initial time point *tet*A concentration). Conformational changes in the pBR322 plasmid during photolysis (D) and quantitative analysis of fluorescence signals of plasmids with different conformations using Image J (C).

plasmid-borne ARGs by disrupting the supercoiled form of the plasmid through heat pretreatment at 75 °C.

HT-qPCR Underestimated the Level of Plasmid-borne ARGs Contamination in the Environment. HT-qPCR is an enhanced version of traditional quantitative PCR. It enables rapid and precise quantitative analysis of hundreds to thousands of samples or target genes simultaneously by incorporating automated equipment, microfluidic chips, or multiwell plate technology.[44] According to the literature, a significant proportion of plasmids in natural water environments exist in supercoiled form, a finding substantiated by our experimental results (Figure S5).[45,46] The quantification of plasmid-borne ARGs using HT-qPCR with standard curve-based calculations may lead to underestimation of their environmental contamination potential. We collected water samples from sampling sites S1, S2, and S3 along the Songhua River, extracted the DNA, and selected 58 ARGs for HT-qPCR detection. Among these, 18 ARGs were undetectable at all three sampling sites. The relative abundance of ARGs (16S rRNA-normalized) in the untreated DNA samples was compared with that in the DNA samples after pretreatment at 75 °C for 10 min. The results showed that, on average, 55.9% of the ARGs exhibited significant enhancement across the three sampling sites, while 34.3% of the ARGs were undetectable before heat treatment but showed higher relative abundance after treatment (Figure 5a and Table S5).

Simultaneously, we observed a reduction in the relative abundance of certain ARGs. To investigate this phenomenon, samples from the S2 sampling site were selected to extract plasmid DNA and conduct HT-qPCR detection (the methodology is detailed in Text S3). The results indicated that ARGs with increased relative abundance are located on plasmids, whereas those with significantly decreased relative abundance were associated with nonplasmid DNA. This suggests that the heat treatment method could potentially lead to the degradation of nonplasmid borne ARGs (Figure 5b and Table S6). In conclusion, our findings indicate that qPCR, when used to directly detect environmental samples of ARGs, significantly underestimates the contamination levels of plasmid-borne ARGs, which are associated with a high risk of dissemination.[23] Heat pretreatment methods can significantly enhance the proportion of quantifiable plasmid, enabling more accurate quantification of ARGs concentrations through standard curves generated using linearized ARGs substrates. Meanwhile, detection of plasmid-borne ARGs in the environment should receive more attention.

■ ENVIRONMENTAL IMPLICATIONS

Accurate Detection of Plasmid-Borne ARGs is Essential for Evaluating Their Potential Risks to Human Health. The human health risk assessment framework for ARGs developed by Zhang et al. includes three assessment criteria: (1) enrichment in human-associated environments, (2) gene mobility, and (3) presence/absence in ESKAPE pathogens (host pathogenicity).[47] Zhang et al. proposed the following classification: ARGs that fail to meet the first criterion are classified as Rank IV (lowest risk), those meeting the first but not the second criterion as Rank III, those meeting the first and second but not the third criterion as Rank II, and those meeting all three criteria as Rank I (highest risk). When ARGs are carried by a plasmid, they are considered mobile, meaning that criterion (2) is met. However, qPCR underestimates the contamination concentration of ARGs borne by supercoiled form plasmids. This implies that these ARGs may not be identified in the environment, potentially leading to Rank II ARGs being misclassified as Rank IV. Therefore, accurate quantification of plasmid-borne ARGs is crucial for assessing their potential risks to human health. Currently, metagenomic sequencing is also used to detect environmental ARGs. Before sequencing environmental DNA samples, the DNA must be fragmented into approximately 350 bp using ultrasound and other methods.[48,49] This pretreatment

https://doi.org/10.1021/acsestwater.5c00272
ACS EST Water 2025, 5, 4025−4034

mitigates the impact of the plasmid structure on the constructed metagenomics library, highlighting the advantages of metagenomics sequencing (i.e., the integrity of the ARGs is not a prerequisite). However, HT-qPCR is likely to remain an important tool in future investigations of ARGs contamination due to its advantages, including high throughput, high specificity, and low cost. Therefore, it is crucial to develop a method that effectively addresses the impact of plasmid structure on qPCR detection.

A Structure Change in Vector Plasmids can Interfere with Data from ARG Degradation Experiments. Given the rising pollution caused by ARGs, various degradation technologies, such as photodegradation and advanced oxidation processes, are being increasingly developed. In experiments aimed at developing ARGs degradation techniques, plasmid-borne ARGs are commonly used as the subjects of study, and it is crucial to consider the potential interference of the plasmid structure in qPCR detection. For instance, in ARGs photodegradation experiments, DNA may undergo direct degradation and indirect photolysis when exposed to simulated sunlight.[50] This DNA damage may result in a structure change in the ARGs vector plasmid.[19] The impact of these changes on the ARGs qPCR assay remains however uncertain. We irradiated the pBR322 plasmid with a 1000 W xenon lamp and measured the *tet*A concentration in the samples using qPCR (Text S4). The concentrations of all measured ARGs were determined using standard curves generated with linearized ARGs vector plasmids as calibration standards. The results indicated that the tetA concentration initially increased, peaked at 4 h, and subsequently decreased (Figure 6a). However, the photodegradation of *tet*A should in theory follow a quasi-first-order kinetic model. Electrophoresis analysis of the photolysis sample of the pBR322 plasmid revealed significant structure changes during the photolysis process (Figure 6d).

Quantitative analysis of the fluorescence signals in the electropherograms using ImageJ software showed that the pBR322 plasmid primarily exhibited a supercoiled form at 0 h. As photolysis progressed, this supercoiled form gradually transitioned to a nicked circular form due to DNA damage caused by light exposure. By 4 h of photolysis, all plasmids had converted to the nicked circular form, coinciding with the peak concentration of *tet*A detected. Continued photolysis further disrupted the plasmid, resulting in the formation of the linear form (Figures 6c and S4). A similar process of structural changes in plasmid conformation was detailed in the study by Shin and Lee.[26] These findings suggest that the structure change in the pBR322 plasmid led to observed variations in the *tet*A concentration. Although *tet*A was progressively photolyzed from 0 to 4 h, the increase in the nicked circular form of the plasmid enhanced the efficiency of *tet*A detection, resulting in an upward trend in *tet*A concentration during the initial photolysis period. After 4 h, when the pBR322 plasmid had fully transitioned to the detectable nicked circular and linear form, the detected *tet*A concentration gradually decreased as photolysis continued.

To address this issue, we treated the photolyzed samples with ApaL I nucleic acid endonuclease, converting all pBR322 plasmids into their linear form. Subsequent qPCR analysis indicated that the *tet*A concentration decreased from 0 h, aligning with the quasi-primary kinetic equation (Figure 6b). Therefore, to prevent interference from the supercoiled form of the plasmid in qPCR detection, it is essential to linearize the ARGs vector plasmid using an appropriate restriction endonuclease, thereby ensuring the accurate detection of ARGs.

CONCLUSIONS

This study demonstrated that plasmid samples containing approximately 90% supercoiled form plasmid could not be directly detected by qPCR. Therefore, we propose a heat pretreatment method that involves heating the plasmid samples at 75 °C for 10 min. This method significantly increased the quantifiable percentage of the *tet*A gene in the pBR322 plasmid from 14.1% to 69.1%. This is attributed to the ability of heat pretreatment to diminish the supercoiled form of the plasmid, thereby increasing the proportion of linear form and single-stranded DNA that can be detected. In this experiment, the method was validated in water samples from the Songhua River in Northeast China, and it was found that the relative abundance of about 56% of the ARGs in the samples was increased after heat pretreatment, suggesting that the use of qPCR for the detection of environmental ARGs may have underestimated the level of contamination of plasmid-borne ARGs. In addition, the study highlighted the interference caused by plasmid structural variations on qPCR quantification of ARGs in degradation experiments, underscoring the critical role of plasmid linearization in optimizing the accuracy of ARGs qPCR assays. Overall, this study provides potential solutions for precise detection of ARGs in environmental contexts.

ASSOCIATED CONTENT

Supporting Information

The Supporting Information is available free of charge at https://pubs.acs.org/doi/10.1021/acsestwater.5c00272.

ARGs RT-qPCR detection (Primer information and qPCR program settings); Environmental sample collection and analysis (sampling point location and ARGs extraction); ARGs relative abundance detection data (PDF)

AUTHOR INFORMATION

Corresponding Author

Ya-nan Zhang − *State Environmental Protection Key Laboratory of Wetland Ecology and Vegetation Restoration, School of Environment, Northeast Normal University, Changchun, Jilin 130024, P. R. China;* orcid.org/0000-0001-9792-0935; Email: zhangyn912@nenu.edu.cn

Authors

Linyi Fan − *State Environmental Protection Key Laboratory of Wetland Ecology and Vegetation Restoration, School of Environment, Northeast Normal University, Changchun, Jilin 130024, P. R. China*

Tingting Zhang − *State Key Laboratory of Pollution Control and Resource Reuse, School of the Environment, Nanjing University, Nanjing 210023, China*

Tong Zhou − *State Environmental Protection Key Laboratory of Wetland Ecology and Vegetation Restoration, School of Environment, Northeast Normal University, Changchun, Jilin 130024, P. R. China*

Hao Yang − *State Environmental Protection Key Laboratory of Wetland Ecology and Vegetation Restoration, School of*

https://doi.org/10.1021/acsestwater.5c00272
ACS EST Water 2025, 5, 4025−4034

Environment, Northeast Normal University, Changchun, Jilin 130024, P. R. China

Fangyuan Cheng − *State Environmental Protection Key Laboratory of Wetland Ecology and Vegetation Restoration, School of Environment, Northeast Normal University, Changchun, Jilin 130024, P. R. China*

Jiao Qu − *State Environmental Protection Key Laboratory of Wetland Ecology and Vegetation Restoration, School of Environment, Northeast Normal University, Changchun, Jilin 130024, P. R. China;* orcid.org/0000-0001-6080-8704

Willie Peijnenburg − *Institute of Environmental Sciences, Leiden University, Leiden 2300 AA, The Netherlands; National Institute of Public Health and the Environment, Center for Safety of Products and Substances, Bilthoven 3720 AA, The Netherlands;* orcid.org/0000-0003-2958-9149

Complete contact information is available at: https://pubs.acs.org/10.1021/acsestwater.5c00272

Notes

The authors declare no competing financial interest.

■ ACKNOWLEDGMENTS

This work was financially supported by the National Natural Science Foundation of China (42422702, 22176030, 42130705, and 42377048) and the Environmental Protection Research Project of Jilin Provincial Department of Ecology and Environment (No. 2024-10).

■ REFERENCES

(1) Kneis, D.; Berendonk, T. U.; Forslund, S. K.; Hess, S. Antibiotic Resistance Genes in River Biofilms: A Metagenomic Approach toward the Identification of Sources and Candidate Hosts. *Environ. Sci. Technol.* **2022**, *56* (21), 14913−14922.

(2) Liang, H.; Zhang, J.; Hu, J.; Li, X.; Li, B. Fluoroquinolone Residues in the Environment Rapidly Induce Heritable Fluoroquinolone Resistance in Escherichia coli. *Environ. Sci. Technol.* **2023**, *57* (12), 4784−4795.

(3) D'Costa, V. M.; King, C. E.; Kalan, L.; Morar, M.; Sung, W. W.; Schwarz, C.; Froese, D.; Zazula, G.; Calmels, F.; Debruyne, R.; et al. Antibiotic resistance is ancient. *Nature* **2011**, *477* (7365), 457−461.

(4) Klein, E. Y.; Van Boeckel, T. P.; Martinez, E. M.; Pant, S.; Gandra, S.; Levin, S. A.; Goossens, H.; Laxminarayan, R. Global increase and geographic convergence in antibiotic consumption between 2000 and 2015. *Proc. Natl. Acad. Sci. U.S.A.* **2018**, *115* (15), E3463−E3470.

(5) Luo, Y.; Mao, D. Q.; Rysz, M.; Zhou, Q.; Zhang, H. J.; Xu, L.; J J Alvarez, P. Trends in antibiotic resistance genes occurrence in the Haihe River, China. *Environ. Sci. Technol.* **2010**, *44* (19), 7220−7225.

(6) Zhuang, M.; Achmon, Y.; Cao, Y.; Liang, X.; Chen, L.; Wang, H.; Siame, B. A.; Leung, K. Y. Distribution of antibiotic resistance genes in the environment. *Environ. Pollut.* **2021**, *285*, 117402.

(7) Zheng, D.; Yin, G.; Liu, M.; Chen, C.; Jiang, Y.; Hou, L.; Zheng, Y. A systematic review of antibiotics and antibiotic resistance genes in estuarine and coastal environments. *Sci. Total Environ.* **2021**, *777*, 146009.

(8) Bengtsson-Palme, J.; Jonsson, V.; Hess, S. What Is the Role of the Environment in the Emergence of Novel Antibiotic Resistance Genes? A Modeling Approach. *Environ. Sci. Technol.* **2021**, *55* (23), 15734−15743.

(9) Soler, N.; Forterre, P. Vesiduction: the fourth way of HGT. *Environ. Microbiol.* **2020**, *22* (7), 2457−2460.

(10) Quintela-Baluja, M.; Frigon, D.; Abouelnaga, M.; Jobling, K.; Romalde, J. L.; Gomez Lopez, M.; Graham, D. W. Dynamics of integron structures across a wastewater network - Implications to resistance gene transfer. *Water Res.* **2021**, *206*, 117720.

(11) Stalder, T.; Barraud, O.; Casellas, M.; Dagot, C.; Ploy, M. C. Integron involvement in environmental spread of antibiotic resistance. *Front. Microbiol.* **2012**, *3*, 119.

(12) Gomathinayagam, S.; Kodiveri Muthukaliannan, G. Dynamics of antibiotic resistance genes in plasmids and bacteriophages. *Crit. Rev. Microbiol.* **2024**, *51*, 219−228.

(13) Conte, D.; Mesa, D.; Jové, T.; Zamparette, C. P.; Sincero, T. C. M.; Palmeiro, J. K.; Dalla-Costa, L. M. Novel Insights into blaGES Mobilome Reveal Extensive Genetic Variation in Hospital Effluents. *Microbiol. Spectr.* **2022**, *10* (4), No. e02469.

(14) Garner, M. M.; Chrambach, A. Resolution of circular, nicked circular and linear DNA, 4.4 kb in length, by electrophoresis in polyacrylamide solutions. *Electrophoresis* **1992**, *13* (3), 176−178.

(15) Wang, S.; Yang, S.; Quispe, E.; Yang, H.; Sanfiorenzo, C.; Rogers, S. W.; Wang, K.; Yang, Y.; Hoffmann, M. R. Removal of Antibiotic Resistant Bacteria and Genes by UV-Assisted Electrochemical Oxidation on Degenerative TiO_2 Nanotube Arrays. *ACS ES&T Eng.* **2021**, *1* (3), 612−622.

(16) Chen, J.; Kadlubar, F. F.; Chen, J. Z. DNA supercoiling suppresses real-time PCR: a new approach to the quantification of mitochondrial DNA damage and repair. *Nucleic Acids Res.* **2007**, *35* (4), 1377−1388.

(17) Tsirkas, I.; Dovrat, D.; Thangaraj, M.; Brouwer, I.; Cohen, A.; Paleiov, Z.; Meijler, M. M.; Lenstra, T.; Aharoni, A. Transcription-replication coordination revealed in single live cells. *Nucleic Acids Res.* **2022**, *50* (4), 2143−2156.

(18) Peng, J.; Pan, Y.; Zhou, Y.; Kong, Q.; Lei, Y.; Lei, X.; Cheng, S.; Zhang, X.; Yang, X. Triplet Photochemistry of Effluent Organic Matter in Degradation of Extracellular Antibiotic Resistance Genes. *Environ. Sci. Technol.* **2023**, *57* (18), 7230−7239.

(19) Zhang, X.; Li, J.; Fan, W. Y.; Yao, M. C.; Yuan, L.; Sheng, G. P. Enhanced Photodegradation of Extracellular Antibiotic Resistance Genes by Dissolved Organic Matter Photosensitization. *Environ. Sci. Technol.* **2019**, *53* (18), 10732−10740.

(20) Yu, Q.; Feng, T.; Yang, J.; Su, W.; Zhou, R.; Wang, Y.; Zhang, H.; Li, H. Seasonal distribution of antibiotic resistance genes in the Yellow River water and tap water, and their potential transmission from water to human. *Environ. Pollut.* **2022**, *292* (Pt A), 118304.

(21) Zhao, Z.; Zhang, K.; Wu, N.; Li, W.; Xu, W.; Zhang, Y.; Niu, Z. Estuarine sediments are key hotspots of intracellular and extracellular antibiotic resistance genes: A high-throughput analysis in Haihe Estuary in China. *Environ. Int.* **2020**, *135*, 105385.

(22) Liu, X.; Xiao, P.; Guo, Y.; Liu, L.; Yang, J. The impacts of different high-throughput profiling approaches on the understanding of bacterial antibiotic resistance genes in a freshwater reservoir. *Sci. Total Environ.* **2019**, *693*, 133585.

(23) Yu, Z.; Wang, Y.; Lu, J.; Bond, P. L.; Guo, J. Nonnutritive sweeteners can promote the dissemination of antibiotic resistance through conjugative gene transfer. *ISME J.* **2021**, *15* (7), 2117−2130.

(24) Vos, S. M.; Tretter, E. M.; Schmidt, B. H.; Berger, J. M. All tangled up: how cells direct, manage and exploit topoisomerase function. *Nat. Rev. Mol. Cell Biol.* **2011**, *12* (12), 827−841.

(25) Ashley, R. E.; Dittmore, A.; McPherson, S. A.; Turnbough, C. L., Jr.; Neuman, K. C.; Osheroff, N. Activities of gyrase and topoisomerase IV on positively supercoiled DNA. *Nucleic Acids Res.* **2017**, *45* (16), 9611−9624.

(26) Shin, S.; Lee, Y. Reaction Kinetics of Singlet Oxygen with an Extracellular Antibiotic Resistance Gene (e-ARG) and Its Implications for the e-ARG Photodegradation Pathway in Sunlit Surface Water. *ACS ES&T Water* **2023**, *3* (9), 3072−3081.

(27) Ahmed, Y.; Lu, J.; Yuan, Z.; Bond, P. L.; Guo, J. Efficient inactivation of antibiotic resistant bacteria and antibiotic resistance genes by photo-Fenton process under visible LED light and neutral pH. *Water Res.* **2020**, *179*, 115878.

(28) Jiang, Q.; Yin, H.; Li, G.; Liu, H.; An, T.; Wong, P. K.; Zhao, H. Elimination of antibiotic-resistance bacterium and its associated/dissociative bla(TEM-1) and aac(3)-II antibiotic-resistance genes in aqueous system via photoelectrocatalytic process. *Water Res.* **2017**, *125*, 219−226.

(29) Hou, Y.; Zhang, H.; Miranda, L.; Lin, S. Serious overestimation in quantitative PCR by circular (supercoiled) plasmid standard: microalgal *pcna* as the model gene. *PLoS One* **2010**, *5* (3), No. e9545.
(30) Irobalieva, R. N.; Fogg, J. M.; Catanese, D. J., Jr.; Sutthibutpong, T.; Chen, M.; Barker, A. K.; Ludtke, S. J.; Harris, S. A.; Schmid, M. F.; Chiu, W.; et al. Structural diversity of supercoiled DNA. *Nat. Commun.* **2015**, *6*, 8440.
(31) King, G. A.; Burla, F.; Peterman, E. J. G.; Wuite, G. J. L. Supercoiling DNA optically. *Proc. Natl. Acad. Sci. U.S.A.* **2019**, *116* (52), 26534−26539.
(32) Lal, A.; Dhar, A.; Trostel, A.; Kouzine, F.; Seshasayee, A. S.; Adhya, S. Genome scale patterns of supercoiling in a bacterial chromosome. *Nat. Commun.* **2016**, *7*, 11055.
(33) Yamaguchi, Y.; Inouye, M. An endogenous protein inhibitor, YjhX (TopAI), for topoisomerase I from Escherichia coli. *Nucleic Acids Res.* **2015**, *43* (21), 10387−10396.
(34) Keller, J. G.; Hymoller, K. M.; Thorsager, M. E.; Hansen, N. Y.; Erlandsen, J. U.; Tesauro, C.; Simonsen, A. K. W.; Andersen, A. B.; Vandso Petersen, K.; Holm, L. L.; et al. Topoisomerase 1 inhibits MYC promoter activity by inducing G-quadruplex formation. *Nucleic Acids Res.* **2022**, *50* (11), 6332−6342.
(35) Rawdon, E. J.; Dorier, J.; Racko, D.; Millett, K. C.; Stasiak, A. How topoisomerase IV can efficiently unknot and decatenate negatively supercoiled DNA molecules without causing their torsional relaxation. *Nucleic Acids Res.* **2016**, *44* (10), 4528−4538.
(36) Zhang, Y.; Chen, J.; He, S.; Xiao, Y.; Liu, A.; Zhang, D.; Li, X. Systematic identification of aberrant non-coding RNAs and their mediated modules in rotator cuff tears. *Front. Mol. Biosci.* **2022**, *9*, 940290.
(37) Dey, D.; Saha, J.; Roy, A. D.; Bhattacharjee, D.; Sinha, S.; Paul, P. K.; Chakraborty, S.; Hussain, S. A. Sensing of DNA conformation based on change in FRET efficiency between laser dyes. *Sens. Actuators, B* **2014**, *204*, 746−753.
(38) Mahmoudi, R.; Feldman, S.; Kisserli, A.; Duret, V.; Tabary, T.; Bertholon, L. A.; Badr, S.; Nonnonhou, V.; Cesar, A.; Neuraz, A.; et al. Inherited and Acquired Decrease in Complement Receptor 1 (CR1) Density on Red Blood Cells Associated with High Levels of Soluble CR1 in Alzheimer's Disease. *Int. J. Mol. Sci.* **2018**, *19* (8), 2175.
(39) Yu, J.; Zhang, Z.; Cao, K.; Huang, X. Visualization of alkali-denatured supercoiled plasmid DNA by atomic force microscopy. *BBRC* **2008**, *374* (3), 415−418.
(40) Yan, L. F.; Iwasaki, H. Thermal denaturation of plasmid DNA observed by atomic force microscopy. *Jpn. J. Appl. Phys.* **2002**, *41* (12), 7556−7559.
(41) Souli, M. P.; Nikitaki, Z.; Puchalska, M.; Brabcová, K. P.; Spyratou, E.; Kote, P.; Efstathopoulos, E. P.; Hada, M.; Georgakilas, A. G.; Sihver, L. Clustered DNA Damage Patterns after Proton Therapy Beam Irradiation Using Plasmid DNA. *Int. J. Mol. Sci.* **2022**, *23* (24), 15606.
(42) Blakeley-Ruiz, J. A.; Erickson, A. R.; Cantarel, B. L.; Xiong, W.; Adams, R.; Jansson, J. K.; Fraser, C. M.; Hettich, R. L. Metaproteomics reveals persistent and phylum-redundant metabolic functional stability in adult human gut microbiomes of Crohn's remission patients despite temporal variations in microbial taxa, genomes, and proteomes. *Microbiome* **2019**, *7* (1), 18.
(43) Ghoshdastidar, D.; Senapati, S. Dehydrated DNA in B-form: ionic liquids in rescue. *Nucleic Acids Res.* **2018**, *46* (9), 4344−4353.
(44) Knight, M. E.; Webster, G.; Perry, W. B.; Baldwin, A.; Rushton, L.; Pass, D. A.; Cross, G.; Durance, I.; Muziasari, W.; Kille, P.; et al. National-scale antimicrobial resistance surveillance in wastewater: A comparative analysis of HT qPCR and metagenomic approaches. *Water Res.* **2024**, *262*, 121989.
(45) Fu, Z. Q.; Guo, M. S.; Zhou, W. Q.; Xiao, J. Differential roles of positive and negative supercoiling in organizing the E. coli genome. *Nucleic Acids Res.* **2024**, *52* (2), 724−737.
(46) Fogg, J. M.; Judge, A. K.; Stricker, E.; Chan, H. L.; Zechiedrich, L. Supercoiling and looping promote DNA base accessibility and coordination among distant sites. *Nat. Commun.* **2021**, *12* (1), 5683.
(47) Zhang, A. N.; Gaston, J. M.; Dai, C. L.; Zhao, S.; Poyet, M.; Groussin, M.; Yin, X.; Li, L. G.; van Loosdrecht, M. C. M.; Topp, E.; et al. An omics-based framework for assessing the health risk of antimicrobial resistance genes. *Nat. Commun.* **2021**, *12* (1), 4765.
(48) De Abreu, V. A. C.; Perdigao, J.; Almeida, S. Metagenomic Approaches to Analyze Antimicrobial Resistance: An Overview. *Front. Genet.* **2021**, *11*, Review.
(49) Greninger, A. L.; Zerr, D. M.; Qin, X.; Adler, A. L.; Sampoleo, R.; Kuypers, J. M.; Englund, J. A.; Jerome, K. R. Rapid Metagenomic Next-Generation Sequencing during an Investigation of Hospital-Acquired Human Parainfluenza Virus 3 Infections. *J. Clin. Microbiol.* **2017**, *55* (1), 177−182.
(50) Zhang, T.; Cheng, F.; Yang, H.; Zhu, B.; Li, C.; Zhang, Y. N.; Qu, J.; Peijnenburg, W. Photochemical degradation pathways of cell-free antibiotic resistance genes in water under simulated sunlight irradiation: Experimental and quantum chemical studies. *Chemosphere* **2022**, *302*, 134879.

https://doi.org/10.1021/acsestwater.5c00272
ACS EST Water 2025, 5, 4025−4034